*Inorg. Chem.* **2008**, *47*, 10945−10952

# Comparison of the Structure and Magnetic Order in a Series of Layered Ni(II) Organophosphonates, Ni[$(RPO_3)(H_2O)$] (R = $C_6H_5$, $CH_3$, $C_{18}H_{37}$)

**Elvira M. Bauer,*,† Carlo Bellitto,† Guido Righini,† Marcello Colapietro,‡ Gustavo Portalone,*,‡ Marc Drillon,§ and Pierre Rabu*,§**

*CNR-Istituto di Struttura della Materia, Via Salaria Km. 29.3, I-00016 Monterotondo Stazione, Rome, Italy, Department of Chemistry, University of Rome "Sapienza", P.le A. Moro 5, 00185 Rome, Italy, and Institut de Physique et Chimie des Materiaux de Strasbourg, UMR7504 CNRS - ULP, 23 rue du Loess, 67034 Strasbourg, France*

Received June 18, 2008

The reaction of nickel chloride with phenyl phosphonic acid under hydrothermal conditions resulted in the isolation of yellow-green single crystals of Ni[$(C_6H_5PO_3)(H_2O)$]. The structure of the compound has been solved by X-ray single-crystal diffraction studies. Ni[$(C_6H_5PO_3)(H_2O)$] crystallizes in the orthorhombic space group $Pmn2_1$ and is isostructural with the Mn(II), Fe(II), and Co(II) analogues. It presents the typical features of the hybrid 2D structures, consisting of alternating inorganic and organic layers. The former are formed by six-coordinated nickel(II) ions bridged by oxygen atoms into the layers. The inorganic layers are capped by the phenyl phosphonate groups, with phenyl groups of two adjacent ligands forming a hydrophobic bilayer region, and van der Waals contacts are established between them. The magnetic properties investigated by means of dc and ac susceptibility measurements point to an AF exchange coupling between nearest neighboring Ni(II) ions. Below 5 K, the compound orders magnetically showing the typical features of a canted antiferromagnet. The magnetic behavior and magnetic dimensionality of Ni[$(C_6H_5PO_3)(H_2O)$] have been fully analyzed and compared to those of the Ni(II) parent compounds Ni[$(RPO_3)(H_2O)$] (where R = $CH_3$, $C_{18}H_{37}$), which exhibit different symmetries of the inorganic layers and lengths of the R groups.

## Introduction

Metal phosphonates, M[$(RPO_3)(H_2O)$][1] (where M is a divalent metal ion, R is an alkyl or aryl group) have been widely studied as ionic exchangers,[2] catalysts,[3] and hosts in intercalation compounds, and more interestingly, they belong to the class of hybrid organic−inorganic layered compounds.[4,5] The latter include tetravalent and divalent metal organophosphonates, whose structures significantly differ. The extensively studied Zr(IV) phosphonates[6] are made of inorganic layers of [$ZrO_6$] chromophores, bridged by [$-PO_3]^{2-}$ groups, and the organic layers consist of bilayers of the R groups belonging to different ligands with van der Waals contacts.[6] The structures of divalent metal phosphonates comprise zigzag inorganic layers, alternating along one direction of the unit cell. The pendent organic R group of the phosphonate ligand lies in the interlamellar space, and two organic layers having van der Waal contacts are interspersed to the inorganic ones. In the inorganic layer,

* To whom correspondence should be addressed. E-mail: elvira.bauer@ism.cnr.it (E.M.B.), g.portalone@caspur.it (G.P.), pierre.rabu@ipcms.u-strasbg.fr (P.R.).
† CNR-Istituto di Struttura della Materia.
‡ University of Rome "Sapienza".
§ UMR7504 CNRS - ULP.

(1) Clearfield, A. *Prog. Inorg. Chem.* **1998**, *47*, 371–510.
(2) Kullberg, L. H.; Clearfield, A. *Solv. Extr. Ion Exch.* **1989**, *7* (3), 527–540.
(3) Centi, G.; Trifirò, F.; Ebner, J. R.; Franchetti, V. M. *Chem. Rev.* **1988**, *88*, 55–80.
(4) (a) Cunningham, D.; Hennelly, P. J. D.; Deeney, T. *Inorg. Chim. Acta* **1979**, *37*, 95–102. (b) Cao, G.; Lee, H.; Lynch, V. M.; Mallouk, T. E. *Inorg. Chem.* **1988**, *27*, 2781–2785. (c) Cao, G.; Mallouck, T. E. *Inorg. Chem.* **1991**, *30*, 1434–1438. (d) Zhang, Y.; Scott, K. J.; Wang, R. C.; Clearfield, A. *Chem. Mater.* **1995**, *5*, 1095–1102.
(5) (a) Johnson, J. W.; Jacobson, A. J.; Butler, W. M.; Rosenthal, S. E.; Brody, J. F.; Lewandowsky, J. T. *J. Am. Chem. Soc.* **1989**, *111*, 381–383. (b) Huan, G.; Jacobson, A. J.; Johnson, J. W.; Corcoran, E. W. *Chem. Mater.* **1990**, *2*, 91–93.
(6) Alberti, G. In *Comprehensive Supramolecular Chemistry*; Atwood, J. L., Davies, J. E. D., Macnicol, D. D., Vogtel, F., Eds.; Pergamon Press: New York, 1996; Vol. *7*, pp 151−187, and references therein.
(7) Bellitto, C. In *Magnetism: Molecules to Materials*; Miller, J. S., Drillon, M., Eds.; Wiley-VCH: Weinheim, 2001; Vol. *2*, pp 425−456.

10.1021/ic801124z CCC: $40.75 
Published on Web 11/01/2008

each metal ion is coordinated by six oxygen atoms with approximately octahedral symmetry, four of them bridging neighboring metal ions.

The two-dimensional character of the inorganic subnetwork favors the exchange interaction between nearest neighbor magnetic ions and, at low temperature, a long-range magnetic ordering.[7]

Recently, several divalent transition metal phosphonates, such as M[$(RPO_3)(H_2O)$], (M = Cr, Mn, Fe, Ni, Co and R = $CH_3$, $C_2H_5$, $C_3H_7$, $C_6H_5$, $C_{18}H_{37}$) or Cr[$H_3N(CH_2)_2PO_3$)-(Cl)$(H_2O)$] and Fe[$(C_{18}H_{37}PO_3)(H_2O)$][7−12] have been prepared and studied, and interestingly, some of them were found to be canted antiferromagnets at low temperatures. Further, we have also recently reported the synthesis and structural characterization of two new Ni(II) *n*-alkylphosphonates, that is, Ni(II) methylphosphonate, Ni[$(CH_3PO_3)$-$(H_2O)$], and Ni(II) octadecylphosphonate, Ni[$(C_{18}H_{37}PO_3)$-$(H_2O)$],[13] and we have shown that the latter orders magnetically at $T_N = 21$ K, while the former does not, at least down to the lowest measured temperature, that is, $T = 5$ K.

In an attempt to clarify the magnetic behavior of these nickel(II) derivatives we have investigated in this paper three members of the series of Ni(II) alkylphosphonates. Here we report the room temperature single-crystal structure of the Ni(II) phenylphosphonate monohydrate Ni[$(C_6H_5PO_3)$-$(H_2O)$] and the magnetic properties of the series of layered organo-phosphonates, Ni[$(RPO_3)(H_2O)$], where R = $CH_3$, $C_6H_5$, and $C_{18}H_{37}$, characterized by different interlayer spacings.

## Experimental Section

**Synthesis. Ni[$(C_6H_5PO_3)(H_2O)$].** This compound was prepared as microcrystalline powder,[14] by a neat reaction between Ni(II) hydroxide and phenylphosphonic acid at high temperature in a sealed thick Pirex tube maintained above the melting point of the acid for a few days. In an attempt to isolate a crystalline material, we used three different methods, that is, (a) from reaction in solution and under reflux; (b) by hydrothermal method at low temperature in presence of an inorganic base; and (c) by hydrothermal reaction at high temperature but without addition of an inorganic base.

The first preparation method starts with an aqueous reaction mixture. $[NiSO_4]6H_2O$ (3.28 g, 12.47 mmol) was dissolved in 17.5 mL of HPLC water, and then the solution was filtered and added to a clean aqueous solution containing ammonium phenylphosphonic salt, prepared by addition of approximately 3 mL of a 30% $NH_4OH$ solution to phenylphosphonic acid (Aldrich Chemical Co., 5 g, 31.64 mmol) in water (25 mL). The resulting reaction mixture was refluxed for 3 days. A pale yellow-green microcrystalline solid was separated by filtration, washed several times with water, and air-dried. Anal. Calcd for Ni[$(C_6H_5PO_3)(H_2O)$]: C, 31.04; H, 3.04. Found: C, 30.67; H, 3.24.

A hydrothermal method was used according to the following conditions. Phenylphosphonic acid was dissolved in 50 mL of deionized water by adding a 1 M NaOH solution until a pH = 7.0 has been reached. $[Ni(NO_3)_2]6H_2O$ (0.58 g, 2 mmol) was added to this aqueous sodium phenylphosphonic salt solution and stirred for about 40 min. The mixture was then placed in a Teflon lined autoclave and heated at 100 °C for two days. A pale yellow-green microcrystalline powder was isolated, rinsed with water, and dried to the air. Anal Calcd. for Ni[$(C_6H_5PO_3)(H_2O)$]: Ni, 25.22; C, 31.04; H, 3.04; P, 13.31; O, 27.49. Found: Ni, 25.32; C, 30.64; H, 2.75; P, 13.37.

Single crystals of Ni(II) phenylphosphonate were obtained by hydrothermal synthesis as follows: Phenylphosphonic acid (0.55 g; 3.5 mmol) was suspended in 17.5 mL of deionized water. $[NiCl_2]\cdot 6H_2O$ (0.83 g, 3.5 mmol) was added to this aqueous phenylphosphonic acid suspension, and the reaction mixture was then placed in a Teflon lined autoclave and heated at 200 °C for seven days. A pale yellow-green crystalline solid was isolated, rinsed with water, and dried in the air.

**Ni[$(RPO_3)(H_2O)$] (R = $CH_3$, $C_{18}H_{37}$).** The synthesis of the above-mentioned Ni(II) phosphonates was done according to the previous reported methods.[13] The purity of the compounds was checked by elemental analysis.

**Characterization.** FT-IR absorption spectra were recorded on a Perkin-Elmer 16F PC spectrophotometer using KBr pellets. UV−vis−NIR absorption spectra were recorded on a Perkin-Elmer 950 spectrophotometer equipped with a diffuse reflectance sphere.

Room temperature X-ray powder diffraction data were recorded on a Seifert XRD-3000 diffractometer, in Bragg−Brentano geometry, equipped with a curved graphite monochromator [$\lambda$(Cu K$\alpha_{1,2}$) = 1.54056/1.5444 Å] and a scintillation detector. The data were collected with a step size of 0.02°, over the range $4 < 2\theta < 80°$. Rietveld structure refinement was done by using the program GSAS.[15,16]

The single-crystal structure of Ni[$(C_6H_5PO_3)(H_2O)$] was carried out from a selected yellow-green tablet of approximately $0.15 \times 0.05 \times 0.05$ mm$^3$. The X-ray intensity data were collected at room temperature on a four-circle diffractometer equipped with a Xcalibur S CCD area detector, graphite monochromator and a Mo K$\alpha$ enhanced fine-focus sealed tube ($\lambda$ = 0.71073 Å). They were corrected for absorption effects by using CrysAlis RED.[17] The structure was solved by using the SIR97 package[17] and refined from the SHELXL-97[18] software.


(8) (a) Altomare, A.; Bellitto, C.; Ibrahim, S. A.; Mahmoud, M. R.; Rizzi, R. *J. Chem. Soc. Dalton* **2000**, 3913–3919. (b) Bellitto, C.; Federici, F.; Altomare, A.; Rizzi, R.; Ibrahim, S. A. *Inorg. Chem.* **2000**, *39*, 1803–1808. (c) Bellitto, C.; Federici, F.; Colapietro, M.; Portalone, G.; Caschera, D. *Inorg. Chem.* **2002**, *41*, 709–714. (d) Léone, P.; Palvadeau, P.; Boubekeur, K.; Meerschaut, A.; Bellitto, C.; Bauer, E. M.; Righini, G.; Fabritchnyi, P. *J. Solid State Chem.* **2005**, *178*, 1125–1132.

(9) (a) Bellitto, C.; Federici, F.; Ibrahim, S. A. *J. Chem. Soc., Chem. Commun.* **1996**, 759–760. (b) Bellitto, C.; Federici, F.; Ibrahim, S. A. *Chem. Mater.* **1998**, *10*, 1076–1082. (c) Bauer, E. M.; Bellitto, C.; Colapietro, M.; Portalone, G.; Righini, G. *Inorg. Chem.* **2003**, *42* (20), 6345–6351.

(10) (a) Bauer, E. M.; Bellitto, C.; Colapietro, M.; Portalone, G.; Ibrahim, S. A.; Mahmoud, M. R.; Righini, G. *J. Solid State Chem.* **2006**, *179*, 389–397. (b) Salami, T. O.; Fan, X.; Zavalij, P. Y.; Oliver, S. R. J. *J. Chem. Soc. Dalton* **2006**, 1574–1578.

(11) (a) Carling, S. G.; Day, P.; Visser, D.; Kremer, R. K. *J. Solid State Chem.* **1993**, *106*, 111–119. (b) Carling, S. G.; Fanucci, G. E.; Talham, D. R.; Visser, D.; Day, P. *Solid State Sci.* **2006**, *8*, 321–325.

(12) Bellitto, C.; Bauer, E. M.; Léone, P.; Righini, G.; Guillot-Deudon, C.; Meerschaut, A. *J. Solid State Chem.* **2006**, *179*, 579–589.

(13) Bellitto, C.; Bauer, E. M.; Ibrahim, S. A.; Mahmoud, M. R.; Righini, G. *Chem. Eur. J.* **2003**, *9*, 1324–1331.

(14) Hix, G. B.; Harris, K. D. M. *J. Mater. Chem.* **1998**, *8*, 579–584.

(15) Larson, A. C.; Von Dreele, R. B. *GSAS: Generalized Structure Analysis System*, Report LAUR 86-748; Los Alamos National Laboratory: Los Alamos, NM, 1994.

(16) Toby, B. H. *J. Appl. Cristallogr.* **2001**, *34*, 210–213.

(17) (a) *CrysAlis CCD and CrysAlis RED*, Versions 1.171.32.3; Oxford Diffraction Ltd.: Abingdon, Oxfordshire, U.K., 2006, 115−119. (b) Altomare, A.; Burla, M. C.; Camalli, M.; Cascarano, G.; Giacovazzo, C.; Guagliardi, A.; Moliterni, A. G. G.; Polidori, G.; Spagna, R. *J. Appl. Crystallogr.* **1999**, *32*, 115. (c) Flack, H. D. *Acta Crystallogr.* **1983**, *A39*, 876–881.

**Table 1.** Crystal Data for Ni[(C$_6$H$_5$PO$_3$)(H$_2$O)]

| | |
|---|---|
| **Crystal Data** | |
| chemical formula | $C_6H_7NiO_4P$ |
| $M_r$ | 229.75 |
| cell setting, space group | orthorhombic, $Pmn2_1$ |
| temperature (K) | 298(2) |
| $a$, $b$, $c$ (Å) | 5.54853(19), 14.3919(5), 4.79766(13) |
| $V$ (Å$^3$) | 383.11(2) |
| $Z$ | 2 |
| $D_x$ (Mg m$^{-3}$) | 1.992 |
| radiation type | Mo Kα, 0.71073 Å |
| $\mu$ (cm$^{-1}$) | 27.1 |
| crystal form, color | tablets, yellow-green |
| crystal size (mm) | 0.15 × 0.05 × 0.05 |
| **Data Collection** | |
| diffractometer | Oxford Diffraction Xcalibur S CCD |
| data collection method | $\omega$ and $\phi$ |
| absorption correction | multiscan (based on symmetry-related measurements) |
| $T_{min}$ | 0.708 |
| $T_{max}$ | 0.873 |
| no. of measured, independent, and observed reflections [$I > 2\sigma(I)$] | 39560, 1467, 1420 |
| criterion for observed reflections | $I > 2\sigma(I)$ |
| $R_{int}$ | 0.027 |
| $\theta_{max}$ (deg) | 32.5 |
| **Refinement** | |
| refinement on | $F^2$ |
| $R[F^2 > 2\sigma(F^2)]$, $wR(F^2)$, $S$ | 0.037, 0.092, 1.12 |
| no. of reflections | 1467 |
| no. of parameters | 94 |
| H-atom treatment | constrained to parent site |
| weighting scheme | calculated $w = 1/[\sigma^2(F_o^2) + (0.0526P)^2 + 0.5711P]$ where $P = (F_o^2 + 2F_c^2)/3$ |
| $(\Delta/\sigma)_{max}$ | <0.0001 |
| $\Delta\rho_{max}$, $\Delta\rho_{min}$ (e Å$^{-3}$) | 0.30, −0.22 |
| Flack parameter | 0.01(2) |

Dc and ac magnetic susceptibility and magnetization measurements were performed by using a Quantum Design MPMS-XL SQUID magnetometer in fields up to 5 T, in the range 1.8−300 K. A cellulose capsule was filled with a freshly prepared polycrystalline sample and placed inside a polyethylene straw at the end of the sample rod. The experimental data were corrected for the core magnetization using Pascal's constants and diamagnetism of the sample holder.

## Crystal Structure

The Ni(II) phenylphosphonate, Ni[(C$_6$H$_5$PO$_3$)(H$_2$O)], is isostructural with the layered compounds M[(C$_6$H$_5$PO$_3$)(H$_2$O)] (M = Fe, Co, Mn).[8,10,11] Details of the crystal data collection, structure solution, and refinement are reported in Table 1. The unit-cell packing of the compound along the *a* axis is shown in Figure 1. The structure is made of inorganic layers perpendicular to the *b* axis (see Figure 2), which are composed of corner-sharing [NiO$_5$(H$_2$O)] octahedra.

The nickel atoms are six-coordinated by five oxygen atoms of the phosphonate groups (O1, O2) and one from the water molecule (O3). Since the compound contains only one phosphonate per metal ion, all the phosphonate oxygen atoms take part in metal binding. Two oxygen atoms (O2) chelate the metal ion and, at the same time, bridge across adjacent metal ions in the same row. Oxygen O1 of the phosphonate

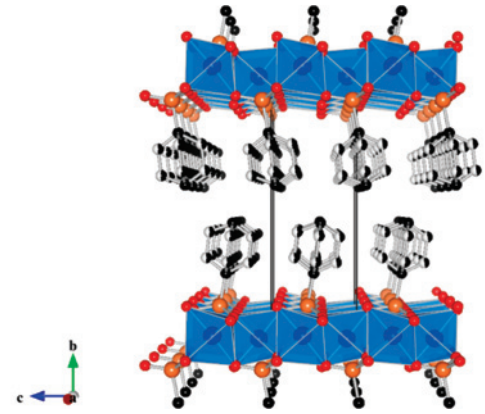


**Figure 1.** Unit-cell packing of Ni[(C$_6$H$_5$PO$_3$)(H$_2$O)] viewed along the *a* axis.

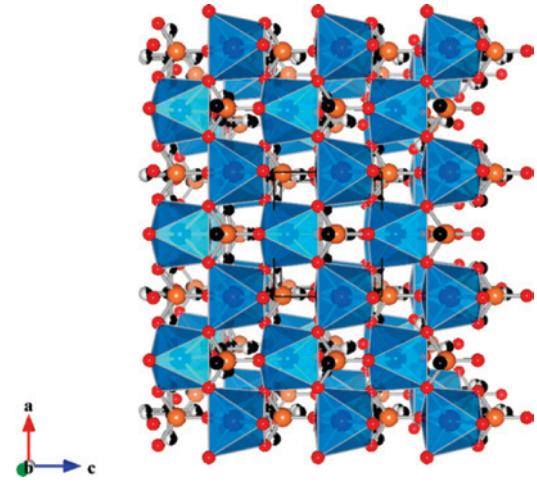


**Figure 2.** Crystal structure of Ni[(C$_6$H$_5$PO$_3$)(H$_2$O)] viewed along the *b* axis; the organic groups are omitted for clarity.

lying in the mirror plane bonds to only one Ni atom, and it is located trans to the oxygen of the water molecule. The octahedron is distorted, and one of the cis O−Ni−O angles is small (56°), while the others range between 83° and 116°. Ni atoms are linked along the *c* axis by the third oxygen of the phosphonate, O2, to form a kinked or crenelated (*ac*) layer. The structure has a mirror plane, and the P−C bond and the plane containing the phenyl ring are nearly perpendicular to the inorganic network between layers. The phenyl ring is disordered between two orientations perpendicular to each other within a single layer. The layers are then translationally related along the *b* axis (see Figure 1). Further, the disorder occurs in the *b*-direction, through stacking disorder or twinning. The comparison of the volume of the unit cell with those of the isostructural Mn(II), Fe(II), and Co(II) compounds ($V_{(Mn)}$ = 402.7 Å$^3$, $V_{(Fe)}$ = 400.8 Å$^3$, $V_{(Co)}$ = 393.44 Å$^3$, and $V_{(Ni)}$ = 383.11 Å$^3$ for metal(II) phenylphosphonate) agrees with the variation of ionic radii of the metal ions.

To check the presence of other phases in the microcrystalline powders of the title compound, X-ray powder diffraction experiment has been performed and the results are reported in Figure S1 (Supporting Information). The Rietveld method analysis of the diffraction profiles confirms the

(18) Sheldrick, G. M. *SHELXL-97, Program for the Refinement of Crystal Structures*; University of Göttingen: Göttingen, Germany; 1997.

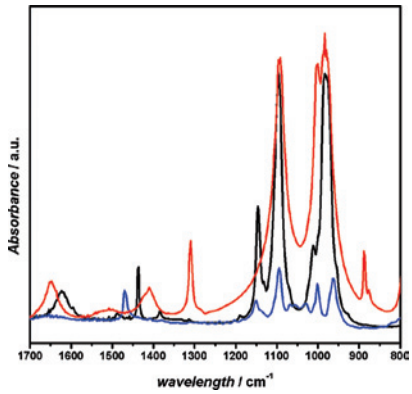


**Figure 3.** FT-IR spectra of (a) Ni[$(C_6H_5PO_3)(H_2O)$] (black line), (b) Ni[$(CH_3PO_3)(H_2O)$] (red line), and (c) Ni[$(C_{18}H_{37}PO_3)(H_2O)$] (blue line) in KBr in the range 1700−800 $cm^{-1}$.

presence of a single phase, namely, the same one of that showed by the single-crystal.

## Optical Properties

The IR spectrum of Ni[$(C_6H_5PO_3)(H_2O)$] together with those of the other two Ni(II) alkyl phosphonates in the range 1700−800 $cm^{-1}$ are displayed in Figure 3. They all feature two intense bands, centered at 3416 $cm^{-1}$ and 3442 $cm^{-1}$, assignable to OH stretching vibrations of the coordinated water molecules. The medium band observed at 1620−1650 $cm^{-1}$ in both the phenyl and methyl compounds is assigned to $H_2O$ bending frequency but is not seen clearly for the octadecyl derivative. The complete conversion of the phosphonic acid is demonstrated by the absence of OH stretching vibrations of the POH group at ∼2700−2550 $cm^{-1}$ and 2350−2100 $cm^{-1}$. Four strong bands due to the [$PO_3$] group vibrations are observed in the range 1200−970 $cm^{-1}$. They are characterized by different relative intensities and degrees of band splitting, the octadecyl derivative, Ni[$(C_{18}H_{37}PO_3)(H_2O)$], showing the bigger ones. Two main bands can be identified: the band at 1095 $cm^{-1}$ is observed in all three phosphonates as a single peak and is assigned to the asymmetric $PO_3^{2-}$ stretching.[19] The stretching bands observed at ∼1000 $cm^{-1}$ and ∼980 $cm^{-1}$ behave differently. The former in fact is present in all three Ni(II) compounds, but with a different intensity, the latter is split into two components and can be assigned to the symmetric $PO_3^{2-}$ stretches. The observed splitting of the band at ∼980 $cm^{-1}$ points to the presence of lower and different local site symmetries.

## Magnetic Properties

**Ni[$(C_6H_5PO_3)(H_2O)$].** The temperature dependence of the molar magnetic susceptibility, measured on a polycrystalline sample at an applied field of 100 Oe, is illustrated in Figures 4 and 5 as $\chi_M = f(T)$ and $\chi_M T = f(T)$, respectively. At high temperature, the magnetic behavior agrees with the Curie−Weiss law [$\chi_M = C/(T - \theta)$], with $C = 1.26$ $cm^3$ K $mol^{-1}$ and $\theta = -22.4$ K. The value of the Curie constant is consistent

(19) Seip, C. T.; Granroth, G. E.; Meisel, M. W.; Talham, D. R. *J. Am. Chem. Soc.* **1997**, *119*, 7084–7094.

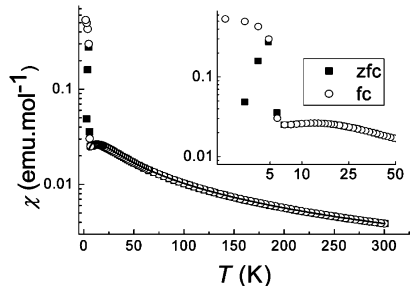


**Figure 4.** ZFC and FC $\chi_M$ vs $T$ plots of Ni[$(C_6H_5PO_3)(H_2O)$] at an applied magnetic field of 100 Oe. Filled squares and open circles represent ZFC and FC measurements, respectively. The inset is a zoom of the low temperature data showing the irreversible magnetization (with a log($T$) scale). The full line represents the best fit to the scaling model described in the text.

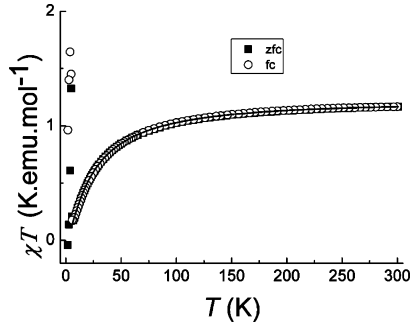


**Figure 5.** $\chi_M T$ vs $T$ plots of Ni[$(C_6H_5PO_3)(H_2O)$] under an applied magnetic field of 100 Oe. Filled squares and open circles represent ZFC and FC measurements, respectively. The full line represents the best fit to the scaling model described in the text.

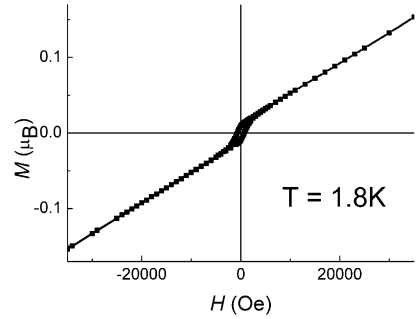


**Figure 6.** Hysteresis loop, $M$ vs $H$, of Ni[$(C_6H_5PO_3)(H_2O)$] at $T = 1.8$ K, showing a coercive field, $H_C$, of 700 Oe.

with the presence of Ni(II) ion in $O_h$ symmetry ($S = 1$, $g = 2.24$) while the negative value of $\theta$ points to predominant AF exchange interactions between spin carriers. As the temperature decreases, $\chi_M$ gradually increases until a maximum at about $T_{max} \approx 11$ K, then decreases, and finally, below 5 K, increases abruptly.

The regular decrease of the $\chi T$ vs $T$ plot from room temperature down to 5 K and then the steep upturn observed is the signature of a canted AF long-range order. The occurrence of weak ferromagnetic state is ascribed for by the out of phase signal in ac susceptibility at $T_N = 5$ K, as shown in Figure S2 (Supporting Information). The latter state is confirmed also by the zero-field cooled (ZFC) and field cooled (FC) magnetization curves ($H = 100$ Oe) and by the field dependence of the magnetization recorded at $T = 1.8$ K (see Figure 6). For $H = 4$ T, the magnetization is about 10% of the expected value for fully aligned spins. The

**Table 2.** Crystal and Magnetic Data of Ni(II) Phosphonates

| compound | space group | unit-cell parameters | | | volume (Å$^3$) | $\theta$ (K) | ordering temperature |
|---|---|---|---|---|---|---|---|
| | | $a$ (Å) | $b$ (Å) | $c$ (Å) | | | |
| $NH_4[Ni(PO_4)(H_2O)]$[a] | $Pmn2_1$ | 5.5698(2) | 8.767(1) | 4.746(1) | 231.75 | −27 | absent[b] |
| $Ni[(CH_3PO_3)(H_2O)]$ | $Pmn2_1$ | 5.587(1) | 8.698(1) | 4.731(1) | 229.91 | −32 | absent[b] |
| $Ni[(C_6H_5PO_3)(H_2O)]$ | $Pmn2_1$ | 5.548(8) | 14.392(1) | 4.798(1) | 383.10 | −25 | $T_N = 5$ K |
| $Ni[(C_{18}H_{37}PO_3)(H_2O)]$ | $Pmn2_1$ | 5.478(8) | 42.31(1) | 4.725(4) | 1095.13 | +20 | $T_C = 20$ K |

[a] Reference 29. [b] Down to 1.8 K.

presence of the weakly ferromagnetic state is due to a canted spin ground-state.[20] The local spins in this configuration are not perfectly antiparallel leading to a net spontaneous magnetization which saturates in a small field. From the plot, we can deduce the values of the remnant magnetization, $M_{rem} = 0.011\ \mu_B$, and of the coercive field, $H_C = 700$ Oe. If we approximate the value of $M_s$ at 1.8 K to $2M_{rem}$ according to the Wohlfarth model,[20,21] the canting angle is estimated to be less than 1°.

The exchange constant, $J$, between neighboring Ni(II) ions within the layers was determined from the high-temperature series expansion[22−24] for a 2D Heisenberg square planar system:[25]

$$\chi_{sp}(T) = \frac{S(S+1)Ng^2{\mu_B}^2}{3k_BT} \times \sum_n a_n x^n \qquad (1)$$

where $N$, $\mu_B$, and $k_B$ have their usual meanings and $x = J/k_BT$. A good description of the susceptibility was obtained between 15 and 300 K for $S = 1$, $g = 2.24$, and $J/k_B = -3.92$ K. It can be emphasized that the resulting $J$ value is larger than the one deduced from the expression available for a 2D Heisenberg system:[24]

$$k_BT(\chi_{max})/|J|S(S+1) = 2.18 \qquad (2)$$

giving $|J|/k_B = 2.52$ K.

Actually, it appears, in the low temperature range, that the limits of the HTS expansion on one hand and the occurrence of a three-dimensional ordering on the other hand make the dimensionality and hence the $J$ determination questionable.

To describe more precisely the system under consideration, we used another approach based on the scaling theory and proposed by Souletie et al. a few years ago.[26−28]

In that model, it was pointed out that, if the power law

$$\chi T = C(1 - T_C/T)^{-y} \qquad (3)$$

with $T_C > 0$, is well appropriate to describe phase transition systems, solutions with $T_C < 0$ have thermodynamically the same legitimacy and therefore are candidates to describe systems, such as 1D or 2D Heisenberg systems,[28] where spin correlations exist but no long-range order takes place at any finite temperature.

We can differentiate the above expression (eq 3) to deduce the equivalent expression:

$$\partial \log(T)/\partial \log(\chi T) = -(T - TC)/\gamma TC \qquad (4)$$

which intersects the temperature axis at a positive, zero, or negative $T_C$ value and the $T = 0$ axis at $\gamma^{-1}$. The limit $T_C = 0$ corresponds to an exponential variation of $\chi T$ leading to a straight line intersecting the axes at their origin. Focusing on the present layered Heisenberg $S = 1$ compound, 2D systems with isotropic interactions show long-range ordering at $T = 0$ only. Finite values of $T_C$ occur when anisotropy is introduced (Ising or Kosterlitz-Thouless case) or in 3D systems.

The plot of $\partial \log(\chi T) = f(T)$ of $Ni[(C_6H_5PO_3)(H_2O)]$ shows a linear variation in the range 50−9 K, below which a singularity is observed due to the occurrence of a long-range ordering (see Figure S3, Supporting Information). From the fit the following parameters are obtained: $T_C = -11.0(9)$ K, $\gamma = 2.0(1)$, and $C = 1.297$ K cm$^3$ mol$^{-1}$, leading to $g = 2.28$. As shown in Figures 4 and 5, this approach leads to a very good description of the magnetic susceptibility in the paramagnetic regime, and accordingly of the correlations between spin carriers within the layers. At higher temperature, the $\partial \log(\chi T) = f(T)$ plot agrees with a linear law intersecting the origin, thus suggesting a 2D character. However, the intrinsic low accuracy of the high temperature data from standard laboratory measuring setup does not allow being conclusive. Finally, the power law variation deduced from this analysis indicates that the magnetic behavior of $Ni[(C_6H_5PO_3)(H_2O)]$ has a strong three-dimensional character, although the magnetic planes are 14.4 Å apart, and a 3D canted antiferromagnetic ordering is stabilized below $T_N = 5$ K. Significant interplane antiferromagnetic interactions through the phenyl layer might explain the higher $|J|$ value deduced from the HTS fit (see above).

**$Ni[(CH_3PO_3)(H_2O)]$ and $Ni[(C_{18}H_{37}PO_3)(H_2O)]$.** These two layered Ni(II) alkyl phosphonates were investigated down to 1.8 K to determine the nature of the magnetic interactions. They are both layered, and the number of carbon atoms in the alkyl chains allows a tuning of the spacing between the inorganic layers from 8.70 Å for $Ni[(CH_3PO_3)(H_2O)]$ to 42.31 Å for $Ni[(C_{18}H_{37}PO_3)(H_2O)]$ (see Table 2). $Ni[(CH_3PO_3)(H_2O)]$ exhibits, like $Ni[(C_6H_5PO_3)(H_2O)]$, a typical antiferromagnetic magnetic behavior, with a maximum of susceptibility at 11.8 K. However, unlike the Ni(II) phenylphosphonate, no spin-canting at the origin of a long-range order was observed down to the lowest accessible temperature, 1.8 K (see Figure 7).

(20) See for example: Carlin, R. L. *Magnetochemistry*; Springer-Verlag: Berlin, 1986; p 149.
(21) See for example: Blundell, S. *Magnetism in Condensed Matter*; Oxford University Press: New York, 2006.
(22) Rushbrooke, G. S.; Baker, G. A.; Wood, P. J. In *Phase Transitions and Critical Phenomena*; Domb, C., Green, M. S., Eds.; Academic Press: New York, 1974; Vol. *III*, Chapter 5.
(23) Yamaji, K.; Kondo, J. *J. Phys. Soc. Japan* **1973**, *35*, 25–32.
(24) Navarro, R. In *Magnetic Properties of Layered Transition Metal Compounds*; de Jongh, L. J., Ed.; Kluwer Academic Publishers: Norwell, MA, 1990; pp 105−190.

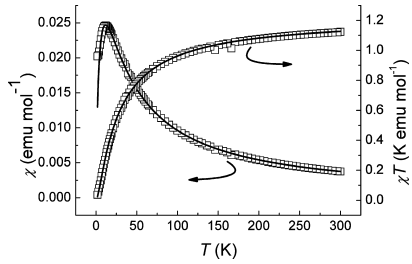


**Figure 7.** Thermal variation of the magnetic susceptibility of Ni[$(CH_3PO_3)(H_2O)$] under an applied magnetic field of 100 Oe. The full line represents the best fit to the scaling model described in the text.

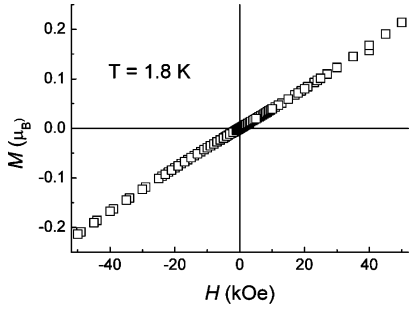


**Figure 8.** Magnetization vs field cycle of Ni[$(CH_3PO_3)(H_2O)$] at $T$ = 1.8 K.

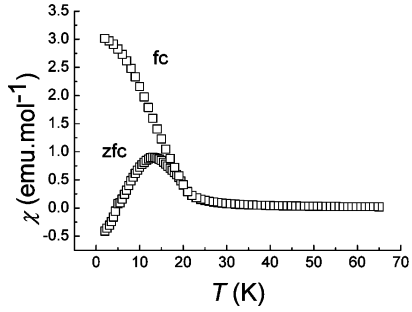


**Figure 9.** $\chi_{zfc}$ and $\chi_{fc}$ vs $T$ plots of Ni[$(C_{18}H_{37}PO_3)(H_2O)$] in the temperature range 5 to 30 K at an applied magnetic field of 50 Oe.

Accordingly, the magnetization vs field plot is characteristic of an antiferromagnet with small magnetization values and slight curvature at high field (see Figure 8). A similar behavior has been reported in the layered Ni(II) derivatives, $NH_4[NiPO_4]H_2O$,[29a] which shows the same crystal space group as the present methyl and phenyl analogues, $Pmn2_1$, and in $H[NiPO_4]H_2O$,[29b] which crystallizes in the monoclinic $P2_1$ space group.

The attempt to describe the magnetic behavior of the title compound by using HTS expansions available for 2D and 1D systems was already reported but was unsuccessful in the low temperature region, when the short-range correlations become efficient.[13] The failure of the 2D approach was explained by the fact that the magnetic layers are not really square planar but strongly corrugated. But, it can also result from fluctuations from the Néel state or different dimensionality. To clarifying this point, we used the above approach derived from the scaling theory and we have plotted $\partial \log(\chi T) = f(T)$, which shows the characteristic power-law variation of $\chi T$ (see Figures S4 and S5, Supporting Information). From this model, a very good fit of the data was obtained over the whole temperature range with the expression (Figure 7)

$$\chi \cdot T = 1.225(1 + 14.3.3/T)^{-1.81} \quad (5)$$

where the prefactor stands for the Curie constant, leading to $g = 2.21$.

As above, a 3D behavior is deduced for this compound, the interplanar distance being shorter (i.e., 8.698 Å) than that observed for the phenyl phosphonate system, which can explain the difficulty to obtain a satisfying fit of the experimental data by using HTS for low-dimensional systems. Interestingly, the critical exponent is similar to that refined for Ni[$(C_6H_5PO_3)(H_2O)$] and is closer to the expected value for a classical system ($S = \infty$, $\gamma = 2$) than a Heisenberg one ($\gamma = 1.387$).

In turn, Ni[$(C_{18}H_{37}PO_3)(H_2O)$] exhibits a ferromagnetic-like behavior, characterized by (a) the divergence between FC and ZFC dc magnetic susceptibility below $T_C = 20$ K (Figure 9) and (b) the onset of an out of phase signal in the ac susceptibility measurements associated to a peak of the in-phase component $\chi'$ (Figure S6, Supporting Information).

Furthermore, the $M$ = M(H) plot at 2 K (Figure S7, Supporting Information) shows a hysteretic behavior with a large coercive field, $H_C = 2500$ Oe, the largest observed in the series, including the canted antiferromagnet Ni[$(C_6H_5PO_3)(H_2O)$]. It is to be noted that the value of the magnetization at 5 T (0.8 $\mu_B$) is less than 40% of that expected for fully aligned $S = 1$ spins. Such behavior can be explained either by a noncollinear antiferromagnetic or a ferrimagnetic ground state.

The temperature dependence of the ZFC $\chi T$ product, after correction of the susceptibility from the demagnetizing factor, $H_d \approx 1/\chi_{max}$,[28,30] was fit with the two exponential expressions used above, $\chi T = C_1 \exp(E_1/kT) + C_2 \exp(E_2/kT)$ for $T > T_C$. A very good result was obtained with $C_1 = 1.07(1)$ K cm$^3$ mol$^{-1}$, $E_1/k = 20.6(8)$ K, $C_2 = 0.0011(2)$ K cm$^3$ mol$^{-1}$, and $E_2/k = 182(4)$ K (Figure 10), indicating that the in-plane magnetic ordering does not obey a single process.

The two exponentials agree with ferromagnetic components, the contributions of which are detailed in the Arrhenius plot in Figure 11. Such a behavior points to a two-dimensional behavior in agreement with the large interplane distance of 42.3 Å, observed for this long alkyl chain derivative. Below $T_N$ a long-range ferromagnetic-type order occurs that can be rationalized,

(25) $x = J/(k_BT)$, $a_0 = 1$, $a_1 = 5.333333333$, $a_2 = 18.66666667$, $a_3 = 56.88888889$, $a_4 = 152.3950631$, $a_5 = 376.9415553$, $a_6 = 918.8538407$, $a_7 = 2134.805724$, and $a_8 = 4572.414518$.

(26) Rabu, P.; Rueff, J. M.; Huang, Z.-L.; Angelov, S.; Souletie, J.; Drillon, M. *Polyhedron* **2001**, *20*, 1677–1685.
(27) Souletie, J.; Rabu, P.; Drillon, M. *Phys. Rev. B* **2005**, *72*, 214427.
(28) Souletie, J.; Drillon, M.; Rabu, P. In *Magnetism: Molecules to Materials*; Miller, J. S., Drillon, M., Eds. Wiley-VCH: Weinheim, 2005; vol. *V*, pp 347−377.
(29) (a) Goni, A.; Pizarro, J. L.; Lezama, L. M.; Barberis, G. E.; Arriortura, M. I.; Rojo, T. *J. Mater. Chem.* **1996**, *6*, 421–427. (b) Goni, A.; Rius, J.; Insausti, M.; Lezama, L. M.; Pizarro, J. L.; Arriortura, M. I.; Rojo, T. *Chem. Mater.* **1996**, *8*, 1052–1060.
(30) Rueff, J.-M.; Paulsen, C.; Souletie, J.; Drillon, M.; Rabu, P. *Solid State Sci.* **2005**, *7*, 431–436.

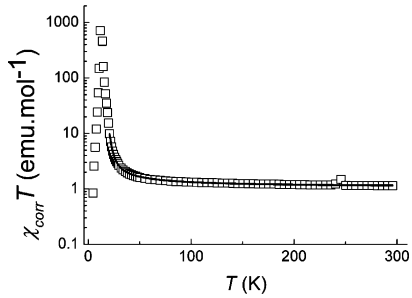


**Figure 10.** Variation of the ZFC magnetic susceptibility of Ni[(C$_{18}$H$_{37}$PO$_3$)(H$_2$O)] as $\chi T$ vs $T$ plot. The full line represents the best fit to the two exponential law described in the text.

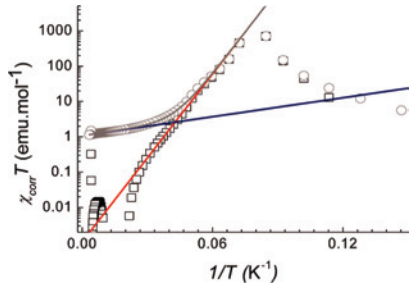


**Figure 11.** Arrhenius ZFC $\chi T$ vs $T^{-1}$ plot of Ni[(C$_{18}$H$_{37}$PO$_3$)(H$_2$O)] showing the best fit (Fit) and the different exponential contributions of the magnetic susceptibility, $\chi T = 1.07 \exp(20.6/T) + 0.0011 \exp(182/T)$ (see text). The blue and red lines represent the first and second term in the expression of $\chi T$. The squares hold for the substraction of the first term from the whole $\chi T$ product (circles).

as due to the existence of efficient dipolar interaction between the Ni(II) magnetic layers.[28,31,32]

## Conclusion

Single crystals of layered Nickel(II) phenylphosphonate Ni[(C$_6$H$_5$PO$_3$)(H$_2$O)] were isolated by heating a mixture of NiCl$_2$ and the phosphonate acid in a hydrothermal bomb for seven days at 200 °C. Unlike most metal phosphonates the crystals were of sufficient size and quality for single-crystal structure determination by X-ray diffraction. The compound is isomorphous and isostructural with the Mn(II), Fe(II), and Co(II) analogues and presents the typical features of a hybrid organic−inorganic structure. The crystal structure consists of inorganic layers of [NiO$_5$(H$_2$O)] octahedra, which share corners via oxygen atoms into a layer. Each of these in-plane oxygens also bond to one P atom and are therefore triply bridged. Since each [NiO$_6$] octahedron connects four octahedra and four phosphonates, the metal:P ratio is 1:1. The fifth and sixth positions of the octahedron are occupied by two out of plane oxygens atoms: one is from the water molecule, and the other is the doubly bridging oxygen that connects to the phosphorus. Each inorganic layer alternates along the *b*-axis with bilayers of phenyl groups bonded to the fourth position of the phosphorus atoms, the latter defining a hydrophobic bilayer region. The phenyl groups are disordered: in one orientation the phenyl group lies in the mirror plane, and in the other orientation it is perpendicular to the plane.

The magnetic properties of this new compound have been investigated together with those of two previously reported Ni(II) alkylphosphonates, that is, Ni[(C$_n$H$_{2n+1}$PO$_3$)(H$_2$O)], $n$ = 1, 18, down to 1.8 K, to have a better understanding of the magnetic behavior of the series.

In spite of having a similar layered structures, the three Ni(II) compounds exhibit different magnetic behaviors depending on the degree of corrugation of the layers, on the interlayer distance, and on the nature of the spacers R. Ni[(CH$_3$PO$_3$)(H$_2$O)] and Ni[(C$_6$H$_5$PO$_3$)(H$_2$O)] show basically antiferromagnetic behavior, whereas the long alkyl chain Ni(II) compound Ni[(C$_{18}$H$_{37}$PO$_3$)(H$_2$O)] is the only of the Ni(II) series showing a ferromagnetic-like behavior in the whole temperature range. In the former, the exchange between the nearest neighboring Ni(II) is antiferromagnetic, as suggested by the negative values of the Weiss constant (see Table 2) and the fit of $\chi$ vs $T$. For the latter, most likely, the ferromagnetic behavior can be related to in-plane distortions of the superexchange pathways, as found previously in Cu(II) alkyl carboxylate hydroxides due to "chemical pressure" induced by the long alkyl chains onto the inorganic sheets.[32,33] These distortions are revealed by the differences in IR spectra in the region of the PO$_3$ group vibrations. They can also be related to the value of the coercive field indicating a higher single ion anisotropy in the case of the long alkyl chain compound.

It is known also that spin canting may be a result of antisymmetric exchange and/or single-ion anisotropy.[20] The structures of the Ni(II) phenyl phosphonate and Ni(II) octadecyl phosphonate compounds satisfy both the requirements. Since the Ni(II) ions are in the same octahedral symmetry in these compounds, the spin canting, where present, should originate from the lack of a symmetric center between adjacent spins. The low value of the critical temperature observed in the former compound and the absence of canting in the methyl phosphonate analogue down to the lowest measured temperature (i.e., $T$ = 1.8 K) could be ascribed to the different degrees of symmetry of the coordinating phosphonate group shown by the various metal alkyl phosphonate compounds and nickel phosphates. The antisymmetric exchange arises from the synergistic effect of local spin−orbit coupling and interactions between the magnetic centers. This effect vanishes when the dinuclear unit is centrosymmetric and when its molecular symmetry is at least $C_{nv}$ ($n > 2$) with the $n$-fold axis running through the interacting centers. It also worth noticing that the isomorphous series of Fe(II) and Mn(II) phosphonates are all canted antiferromagnets, while the isomorphous Co(II) series is antiferromagnetic. Canting can occur either between the layers as found in the very anisotropic layered compound Co(OH)$_2$tp[34,35] or within the layers. In these two nickel compounds, the canting can be ascribed to the distortions induced by the ligands in the structure.

The dimensionality of these magnetic systems was also investigated by using an appropriate scaling model. As

(31) Panissod, P.; Drillon, M. *J. Magn. Magn. Mater.* **1998**, *188*, 93–99.
(32) Rabu, P.; Drillon, M.; Awaga, K.; Fujita, W.; Sekine, T. In *Magnetism: Molecules to Materials*; Miller, J. S., Drillon, M., Eds.; Wiley-VCH: Weinheim, 2002; Vol. 2, pp 357−395.
(33) Fujita, W.; Awaga, K.; Yokoyama, T. *Inorg. Chem.* **1997**, *36*, 196–199.

expected, the compound with the smallest interlayer distance, that is, Ni[$CH_3PO_3$)($H_2O$)], shows a strongly 3D character, whereas the Ni(II) octadecyl phosphonate is mainly 2D as a consequence of the large separation between the magnetic layers generated by the long carbon chain. In addition, the compound Ni[($C_6H_5PO_3$)($H_2O$)] with an intermediate interplanar distance of 14.39 Å has different dimensionality. The fact that the phenyl analogue has a pronounced 3D character suggests that the $\pi$-system in between the layers participates significantly to the interplane coupling, contrarily to the saturated alkylphosphonates.[26,32,36]

Such relationship between structural and magnetic properties was already recently reported in a series of copper and manganese carboxylates.[26,36,37] Work is currently in progress to develop the synthesis routes for obtaining well crystallized samples appropriate for structural analysis.

**Acknowledgment.** This work is supported by MIUR FIRB 2001 program. The Consiglio Nazionale delle Ricerche (Italy) and the European COST Action D35-WG11 are also acknowledged. M.C. and G.P. thank MIUR for 2006 financial support of the project "X-ray diffractometry and spectrometry". We thank also CNRS, France, and University Louis Pasteur, Strasbourg, France, for financial support.

**Supporting Information Available:** Additional structural and magnetic characterization of Ni[($C_6H_5PO_3$)($H_2O$)], Ni[($CH_3PO_3$)-($H_2O$)], and Ni[($C_{18}H_{37}PO_3$)($H_2O$)] and complete X-ray crystallographic files in CIF format for Ni[($C_6H_5PO_3$)($H_2O$)]. This material is available free of charge via the Internet at http://pubs.acs.org.

IC801124Z

(34) Huang, Z.-L.; Drillon, M.; Masciocchi, N.; Sironi, A.; Zhao, J.-T.; Rabu, P.; Panissod, P. *Chem. Mater.* **2000**, *12*, 2805–2812.
(35) Feyerherm, R.; Loose, A.; Rabu, P.; Drillon, M. *Solid State Sci.* **2003**, *5*, 321–326.
(36) Hornick, C.; Rabu, P.; Drillon, M. *Polyhedron* **2000**, *19*, 259–266.
(37) Zheng, Y.-Z.; Xue, W.; Zheng, S.-L.; Tong, M.-L.; Chen, X.-M. *Adv. Mater.* **2008**, *20*, 1534–1538.